



5-1-2023

Constraining High-energy Neutrino Emission from Supernovae with IceCube

R. Abbasi

Loyola University of Chicago

M. Ackermann

Deutsches Elektronen-Synchrotron (DESY)

J. Adams

University of Canterbury

S. K. Agarwalla

University of Wisconsin-Madison

J. A. Aguilar

Université Libre de Bruxelles

See next page for additional authors

Follow this and additional works at: https://ecommons.luc.edu/physics_facpubs

Recommended Citation

Abbasi, R.; Ackermann, M.; Adams, J.; Agarwalla, S. K.; Aguilar, J. A.; Ahlers, M.; Alameddine, J. M.; Amin, N. M.; Andeen, K.; Anton, G.; Argüelles, C.; Ashida, Y.; Athanasiadou, S.; Axani, S. N.; Bai, X.; A. Balagopal, V.; Baricevic, M.; Barwick, S. W.; Basu, V.; Bay, R.; Beatty, J. J.; Becker, K. H.; Tjus, J. Becker; Beise, J.; and Bellenghi, C., "Constraining High-energy Neutrino Emission from Supernovae with IceCube" (2023). *Physics: Faculty Publications and Other Works*. 70. https://ecommons.luc.edu/physics_facpubs/70

This Article is brought to you for free and open access by the Faculty Publications and Other Works by Department at Loyola eCommons. It has been accepted for inclusion in Physics: Faculty Publications and Other Works by an authorized administrator of Loyola eCommons. For more information, please contact ecommons@luc.edu.

Authors

R. Abbasi, M. Ackermann, J. Adams, S. K. Agarwalla, J. A. Aguilar, M. Ahlers, J. M. Alameddine, N. M. Amin, K. Andeen, G. Anton, C. Argüelles, Y. Ashida, S. Athanasiadou, S. N. Axani, X. Bai, V. A. Balagopal, M. Baricevic, S. W. Barwick, V. Basu, R. Bay, J. J. Beatty, K. H. Becker, J. Becker Tjus, J. Beise, and C. Bellenghi



Constraining High-energy Neutrino Emission from Supernovae with IceCube

R. Abbasi¹, M. Ackermann², J. Adams³, S. K. Agarwalla^{4,65}, J. A. Aguilar⁵, M. Ahlers⁶, J. M. Alameddine⁷, N. M. Amin⁸, K. Andeen⁹, G. Anton¹⁰, C. Argüelles¹¹, Y. Ashida⁴, S. Athanasiadou², S. N. Axani⁸, X. Bai¹², A. Balagopal V.⁴, M. Baricevic⁴, S. W. Barwick¹³, V. Basu⁴, R. Bay¹⁴, J. J. Beatty^{15,16}, K.-H. Becker¹⁷, J. Becker Tjus^{18,66}, J. Beise¹⁹, C. Bellenghi²⁰, S. BenZvi²¹, D. Berley²², E. Bernardini²³, D. Z. Besson²⁴, G. Binder^{14,25}, D. Bindig¹⁷, E. Blaufuss²², S. Blot², F. Bontempo²⁶, J. Y. Book¹¹, C. Boscolo Meneguolo²³, S. Böser²⁷, O. Botner¹⁹, J. Böttcher²⁸, E. Bourbeau⁶, J. Braun⁴, B. Brinson²⁹, J. Brostean-Kaiser², R. T. Burley³⁰, R. S. Busse³¹, D. Butterfield⁴, M. A. Campana³², K. Carloni¹¹, E. G. Carnie-Bronca³⁰, S. Chattopadhyay^{4,65}, C. Chen²⁹, Z. Chen³³, D. Chirkin⁴, S. Choi³⁴, B. A. Clark²², L. Classen³¹, A. Coleman¹⁹, G. H. Collin³⁵, A. Connolly^{15,16}, J. M. Conrad³⁵, P. Coppin³⁶, P. Correa³⁶, S. Countryman³⁷, D. F. Cowen^{38,39}, P. Dave²⁹, C. De Clercq³⁶, J. J. DeLaunay⁴⁰, D. Delgado López¹¹, H. Dembinski⁸, K. Deoskar⁴¹, A. Desai⁴, P. Desiati⁴, K. D. de Vries³⁶, G. de Wasseige⁴², T. DeYoung⁴³, A. Diaz³⁵, J. C. Díaz-Vélez⁴, M. Dittmer³¹, A. Domi¹⁰, H. Dujmovic⁴, M. A. DuVernois⁴, T. Ehrhardt²⁷, P. Eller²⁰, R. Engel^{26,44}, H. Erpenbeck⁴, J. Evans²², P. A. Evenson⁸, K. L. Fan²², K. Fang⁴, A. R. Fazely⁴⁵, A. Fedynitch⁴⁶, N. Feigl⁴⁷, S. Fiedlschuster¹⁰, C. Finley⁴¹, L. Fischer², D. Fox³⁸, A. Franckowiak¹⁸, E. Friedman²², A. Fritz²⁷, P. Fürst²⁸, T. K. Gaisser⁸, J. Gallagher⁴⁸, E. Ganster²⁸, A. Garcia¹¹, S. Garrappa², L. Gerhardt²⁵, A. Ghadimi⁴⁰, C. Glaser¹⁹, T. Glauch²⁰, T. Glüsenkamp^{10,19}, N. Goehle⁴⁴, J. G. Gonzalez⁸, S. Goswami⁴⁰, D. Grant⁴³, S. J. Gray²², S. Griffin⁴, S. Griswold²¹, C. Günther²⁸, P. Gutjahr⁷, C. Haack²⁰, A. Hallgren¹⁹, R. Halliday⁴³, L. Halve²⁸, F. Halzen⁴, H. Hamdaoui³³, M. Ha Minh²⁰, K. Hanson⁴, J. Hardin³⁵, A. A. Harnisch⁴³, P. Hatch⁴⁹, A. Haungs²⁶, K. Helbing¹⁷, J. Hellrung¹⁸, F. Henningsen²⁰, L. Heuermann²⁸, S. Hickford¹⁷, A. Hidvegi⁴¹, C. Hill⁵⁰, G. C. Hill³⁰, K. D. Hoffman²², K. Hoshina^{4,67}, W. Hou²⁶, T. Huber²⁶, K. Hultqvist⁴¹, M. Hünnefeld⁷, R. Hussain⁴, K. Hymon⁷, S. In³⁴, N. Iovine⁵, A. Ishihara⁵⁰, M. Jacquart⁴, M. Jansson⁴¹, G. S. Japaridze⁵¹, K. Jayakumar^{4,65}, M. Jeong³⁴, M. Jin¹¹, B. J. P. Jones⁵², D. Kang²⁶, W. Kang³⁴, X. Kang³², A. Kappes³¹, D. Kappesser²⁷, L. Kardum⁷, T. Karg², M. Karl²⁰, A. Karle⁴, U. Katz¹⁰, M. Kauer⁴, J. L. Kelley⁴, A. Khatem Zathul⁴, A. Kheirandish^{53,54}, K. Kin⁵⁰, J. Kiryluk³³, S. R. Klein^{14,25}, A. Kochocki⁴³, R. Koirala⁸, H. Kolanoski⁴⁷, T. Kontrimas²⁰, L. Köpke²⁷, C. Kopper⁴³, D. J. Koskinen⁶, P. Koundal²⁶, M. Kovacevich³², M. Kowalski^{2,47}, T. Kozynets⁶, K. Kruiswijk⁴², E. Krupczak⁴³, A. Kumar², E. Kun¹⁸, N. Kurahashi³², N. Lad², C. Lagunas Gualda², M. Lamoureux⁴², M. J. Larson²², F. Lauber¹⁷, J. P. Lazar^{4,11}, J. W. Lee³⁴, K. Leonard DeHolton^{38,39}, A. Leszczyńska⁸, M. Lincetto¹⁸, Q. R. Liu⁴, M. Liubarska⁵⁵, E. Lohfink²⁷, C. Love³², C. J. Lozano Mariscal³¹, L. Lu⁴, F. Lucarelli⁵⁶, A. Ludwig⁵⁷, W. Luszczak^{15,16}, Y. Lyu^{14,25}, W. Y. Ma², J. Madsen⁴, K. B. M. Mahn⁴³, Y. Makino⁴, S. Mancina^{4,23}, W. Marie Sainte⁴, I. C. Mariş⁵, S. Marka³⁷, Z. Marka³⁷, M. Marsee⁴⁰, I. Martinez-Soler¹¹, R. Maruyama⁵⁸, F. Mayhew⁴³, T. McElroy⁵⁵, F. McNally⁵⁹, J. V. Mead⁶, K. Meagher⁴, S. Mechbal², A. Medina¹⁶, M. Meier⁵⁰, S. Meighen-Berger²⁰, Y. Merckx³⁶, L. Merten¹⁸, J. Micallef⁴³, D. Mockler⁵, T. Montaruli⁵⁶, R. W. Moore⁵⁵, Y. Morii⁵⁰, R. Morse⁴, M. Moulai⁴, T. Mukherjee²⁶, R. Naab², R. Nagai⁵⁰, M. Nakos⁴, U. Naumann¹⁷, J. Necker², M. Neumann³¹, H. Niederhausen⁴³, M. U. Nisa⁴³, A. Noell²⁸, S. C. Nowicki⁴³, A. Obertacke Pollmann¹⁷, V. O'Dell⁴, M. Oehler²⁶, B. Oeyen⁶⁰, A. Olivas²², R. Orsoe²⁰, J. Osborn⁴, E. O'Sullivan¹⁹, H. Pandya⁸, N. Park⁴⁹, G. K. Parker⁵², E. N. Paudel⁸, L. Paul⁹, C. Pérez de los Heros¹⁹, J. Peterson⁴, S. Philippen²⁸, S. Pieper¹⁷, A. Pizzuto⁴, M. Plum¹², Y. Popovych²⁷, M. Prado Rodriguez⁴, B. Pries⁴³, R. Procter-Murphy²², G. T. Przybylski²⁵, C. Raab⁵, J. Rack-Helleis²⁷, K. Rawlins⁶¹, Z. Rechav⁴, A. Rehman⁸, P. Reichherzer¹⁸, G. Renzi⁵, E. Resconi²⁰, S. Reusch², W. Rhode⁷, M. Richman³², B. Riedel⁴, E. J. Roberts³⁰, S. Robertson^{14,25}, S. Rodan³⁴, G. Roellinghoff³⁴, M. Rongen²⁷, C. Rott^{34,62}, T. Ruhe⁷, L. Ruohan²⁰, D. Ryckbosch⁶⁰, I. Safa^{4,11}, J. Saffer⁴⁴, D. Salazar-Gallegos⁴³, P. Sampathkumar²⁶, S. E. Sanchez Herrera⁴³, A. Sandrock⁷, M. Santander⁴⁰, S. Sarkar⁵⁵, S. Sarkar⁶³, J. Savelberg²⁸, P. Savina⁴, M. Schaufel²⁸, H. Schieler²⁶, S. Schindler¹⁰, B. Schlüter³¹, T. Schmidt²², J. Schneider¹⁰, F. G. Schröder^{8,26}, L. Schumacher²⁰, G. Schwefer²⁸, S. Sclafani³², D. Seckel⁸, S. Seunarine⁶⁴, A. Sharma¹⁹, S. Shefali⁴⁴, N. Shimizu⁵⁰, M. Silva⁴, B. Skrzypek¹¹, B. Smithers⁵², R. Snihur⁴, J. Soedingrekso⁷, A. Sjøgaard⁶, D. Soldin⁴⁴, G. Sommani¹⁸, C. Spannfellner²⁰, G. M. Spiczak⁶⁴, C. Spiering², M. Stamatikos¹⁶, T. Stanev⁸, A. Stasik², R. Stein², T. Stezelberger²⁵, T. Stürwald¹⁷, T. Stuttard⁶, G. W. Sullivan²², I. Taboada²⁹, S. Ter-Antonyan⁴⁵, W. G. Thompson¹¹, J. Thwaites⁴, S. Tilav⁸, K. Tollefson⁴³, C. Tönnis³⁴, S. Toscano⁵, D. Tosi⁴, A. Tretin², C. F. Tung²⁹, R. Turcotte²⁶, J. P. Twagirayezu⁴³, B. Ty⁴, M. A. Unland Elorrieta³¹, A. K. Upadhyay^{4,65}, K. Upshaw⁴⁵, N. Valtonen-Mattila¹⁹, J. Vandenbroucke⁴, N. van Eijndhoven³⁶, D. Vannerom³⁵, J. van Santen², J. Vara³¹, J. Veitch-Michaelis⁴, M. Venugopal²⁶, S. Verpoest⁶⁰, D. Veske³⁷, C. Walck⁴¹, T. B. Watson⁵², C. Weaver⁴³, P. Weigel³⁵, A. Weindl²⁶, J. Weldert^{38,39}, C. Wendt⁴, J. Werthebach⁷, M. Weyrauch²⁶, N. Whitehorn^{43,57}, C. H. Wiebusch²⁸, N. Willey⁴³, D. R. Williams⁴⁰, M. Wolf²⁰, G. Wrede¹⁰, J. Wulff¹⁸, X. W. Xu⁴⁵, J. P. Yanez⁵⁵, E. Yildizci⁴, S. Yoshida⁵⁰, F. Yu¹¹, S. Yu⁴³, T. Yuan⁴, Z. Zhang³³, and P. Zhelnin¹¹

IceCube Collaboration⁶⁵¹ Department of Physics, Loyola University Chicago, Chicago, IL 60660, USA² Deutsches Elektronen-Synchrotron DESY, Platanenallee 6, D-15738 Zeuthen, Germany³ Dept. of Physics and Astronomy, University of Canterbury, Private Bag 4800, Christchurch, New Zealand

- ⁴ Dept. of Physics and Wisconsin IceCube Particle Astrophysics Center, University of Wisconsin-Madison, Madison, WI 53706, USA
- ⁵ Université Libre de Bruxelles, Science Faculty CP230, B-1050 Brussels, Belgium
- ⁶ Niels Bohr Institute, University of Copenhagen, DK-2100 Copenhagen, Denmark
- ⁷ Dept. of Physics, TU Dortmund University, D-44221 Dortmund, Germany
- ⁸ Bartol Research Institute and Dept. of Physics and Astronomy, University of Delaware, Newark, DE 19716, USA
- ⁹ Department of Physics, Marquette University, Milwaukee, WI 53201, USA
- ¹⁰ Erlangen Centre for Astroparticle Physics, Friedrich-Alexander-Universität Erlangen-Nürnberg, D-91058 Erlangen, Germany
- ¹¹ Department of Physics and Laboratory for Particle Physics and Cosmology, Harvard University, Cambridge, MA 02138, USA
- ¹² Physics Department, South Dakota School of Mines and Technology, Rapid City, SD 57701, USA
- ¹³ Dept. of Physics and Astronomy, University of California, Irvine, CA 92697, USA
- ¹⁴ Dept. of Physics, University of California, Berkeley, CA 94720, USA
- ¹⁵ Dept. of Astronomy, Ohio State University, Columbus, OH 43210, USA
- ¹⁶ Dept. of Physics and Center for Cosmology and Astro-Particle Physics, Ohio State University, Columbus, OH 43210, USA
- ¹⁷ Dept. of Physics, University of Wuppertal, D-42119 Wuppertal, Germany
- ¹⁸ Fakultät für Physik & Astronomie, Ruhr-Universität Bochum, D-44780 Bochum, Germany
- ¹⁹ Dept. of Physics and Astronomy, Uppsala University, Box 516, SE-75120 Uppsala, Sweden
- ²⁰ Physik-department, Technische Universität München, D-85748 Garching, Germany
- ²¹ Dept. of Physics and Astronomy, University of Rochester, Rochester, NY 14627, USA
- ²² Dept. of Physics, University of Maryland, College Park, MD 20742, USA
- ²³ Dipartimento di Fisica e Astronomia Galileo Galilei, Università Degli Studi di Padova, I-35122 Padova PD, Italy
- ²⁴ Dept. of Physics and Astronomy, University of Kansas, Lawrence, KS 66045, USA
- ²⁵ Lawrence Berkeley National Laboratory, Berkeley, CA 94720, USA
- ²⁶ Karlsruhe Institute of Technology, Institute for Astroparticle Physics, D-76021 Karlsruhe, Germany
- ²⁷ Institute of Physics, University of Mainz, Staudinger Weg 7, D-55099 Mainz, Germany
- ²⁸ III. Physikalisches Institut, RWTH Aachen University, D-52056 Aachen, Germany
- ²⁹ School of Physics and Center for Relativistic Astrophysics, Georgia Institute of Technology, Atlanta, GA 30332, USA
- ³⁰ Department of Physics, University of Adelaide, Adelaide, 5005, Australia
- ³¹ Institut für Kernphysik, Westfälische Wilhelms-Universität Münster, D-48149 Münster, Germany
- ³² Dept. of Physics, Drexel University, 3141 Chestnut Street, Philadelphia, PA 19104, USA
- ³³ Dept. of Physics and Astronomy, Stony Brook University, Stony Brook, NY 11794-3800, USA
- ³⁴ Dept. of Physics, Sungkyunkwan University, Suwon 16419, Republic of Korea
- ³⁵ Dept. of Physics, Massachusetts Institute of Technology, Cambridge, MA 02139, USA
- ³⁶ Vrije Universiteit Brussel (VUB), Dienst ELEM, B-1050 Brussels, Belgium
- ³⁷ Columbia Astrophysics and Nevis Laboratories, Columbia University, New York, NY 10027, USA
- ³⁸ Dept. of Astronomy and Astrophysics, Pennsylvania State University, University Park, PA 16802, USA
- ³⁹ Dept. of Physics, Pennsylvania State University, University Park, PA 16802, USA
- ⁴⁰ Dept. of Physics and Astronomy, University of Alabama, Tuscaloosa, AL 35487, USA
- ⁴¹ Oskar Klein Centre and Dept. of Physics, Stockholm University, SE-10691 Stockholm, Sweden
- ⁴² Centre for Cosmology, Particle Physics and Phenomenology—CP3, Université catholique de Louvain, Louvain-la-Neuve, Belgium
- ⁴³ Dept. of Physics and Astronomy, Michigan State University, East Lansing, MI 48824, USA
- ⁴⁴ Karlsruhe Institute of Technology, Institute of Experimental Particle Physics, D-76021 Karlsruhe, Germany
- ⁴⁵ Dept. of Physics, Southern University, Baton Rouge, LA 70813, USA
- ⁴⁶ Institute of Physics, Academia Sinica, Taipei, 11529, Taiwan
- ⁴⁷ Institut für Physik, Humboldt-Universität zu Berlin, D-12489 Berlin, Germany
- ⁴⁸ Dept. of Astronomy, University of Wisconsin-Madison, Madison, WI 53706, USA
- ⁴⁹ Dept. of Physics, Engineering Physics, and Astronomy, Queen's University, Kingston, ON K7L 3N6, Canada
- ⁵⁰ Dept. of Physics and The International Center for Hadron Astrophysics, Chiba University, Chiba 263-8522, Japan
- ⁵¹ CTSPS, Clark-Atlanta University, Atlanta, GA 30314, USA
- ⁵² Dept. of Physics, University of Texas at Arlington, 502 Yates St., Science Hall Rm 108, Box 19059, Arlington, TX 76019, USA
- ⁵³ Department of Physics & Astronomy, University of Nevada, Las Vegas, NV 89154, USA
- ⁵⁴ Nevada Center for Astrophysics, University of Nevada, Las Vegas, NV 89154, USA
- ⁵⁵ Dept. of Physics, University of Alberta, Edmonton, Alberta, T6G 2E1, Canada
- ⁵⁶ Département de physique nucléaire et corpusculaire, Université de Genève, CH-1211 Genève, Switzerland
- ⁵⁷ Department of Physics and Astronomy, UCLA, Los Angeles, CA 90095, USA
- ⁵⁸ Dept. of Physics, Yale University, New Haven, CT 06520, USA
- ⁵⁹ Department of Physics, Mercer University, Macon, GA 31207-0001, USA
- ⁶⁰ Dept. of Physics and Astronomy, University of Gent, B-9000 Gent, Belgium
- ⁶¹ Dept. of Physics and Astronomy, University of Alaska Anchorage, 3211 Providence Dr., Anchorage, AK 99508, USA
- ⁶² Department of Physics and Astronomy, University of Utah, Salt Lake City, UT 84112, USA
- ⁶³ Dept. of Physics, University of Oxford, Parks Road, Oxford OX1 3PU, UK
- ⁶⁴ Dept. of Physics, University of Wisconsin, River Falls, WI 54022, USA

Received 2023 March 3; revised 2023 May 2; accepted 2023 May 5; published 2023 May 22

⁶⁵ analysis@icecube.wisc.edu

⁶⁶ Also at Institute of Physics, Sachivalaya Marg, Sainik School Post, Bhubaneswar 751005, India.

⁶⁷ Also at Department of Space, Earth and Environment, Chalmers University of Technology, 412 96 Gothenburg, Sweden.

⁶⁸ Also at Earthquake Research Institute, University of Tokyo, Bunkyo, Tokyo 113-0032, Japan.



Abstract

Core-collapse supernovae are a promising potential high-energy neutrino source class. We test for correlation between seven years of IceCube neutrino data and a catalog containing more than 1000 core-collapse supernovae of types IIn and IIP and a sample of stripped-envelope supernovae. We search both for neutrino emission from individual supernovae as well as for combined emission from the whole supernova sample, through a stacking analysis. No significant spatial or temporal correlation of neutrinos with the cataloged supernovae was found. All scenarios were tested against the background expectation and together yield an overall p -value of 93%; therefore, they show consistency with the background only. The derived upper limits on the total energy emitted in neutrinos are 1.7×10^{48} erg for stripped-envelope supernovae, 2.8×10^{48} erg for type IIP, and 1.3×10^{49} erg for type IIn SNe, the latter disfavoring models with optimistic assumptions for neutrino production in interacting supernovae. We conclude that stripped-envelope supernovae and supernovae of type IIn do not contribute more than 14.6% and 33.9%, respectively, to the diffuse neutrino flux in the energy range of about $[10^3\text{--}10^5]$ GeV, assuming that the neutrino energy spectrum follows a power-law with an index of -2.5 . Under the same assumption, we can only constrain the contribution of type IIP SNe to no more than 59.9%. Thus, core-collapse supernovae of types IIn and stripped-envelope supernovae can both be ruled out as the dominant source of the diffuse neutrino flux under the given assumptions.

Unified Astronomy Thesaurus concepts: [Neutrino astronomy \(1100\)](#); [Core-collapse supernovae \(304\)](#); [Circumstellar matter \(241\)](#); [High-energy astrophysics \(739\)](#)

1. Introduction

IceCube has detected a diffuse flux of high-energy astrophysical neutrinos (Aartsen et al. 2013, 2015). The majority of the high-energy neutrinos follow an isotropic distribution, which suggests an extragalactic origin. The active galaxy NGC 1068 was recently reported to be the first extragalactic point source of high-energy neutrinos beyond the 4σ level (IceCube Collaboration et al. 2022). While there is evidence that gamma-ray blazars and tidal disruption events (TDEs) produce high-energy neutrinos (Aartsen et al. 2018a, 2018b; Stein et al. 2021; Reusch et al. 2022), the rate of observed coincidences constrains the overall diffuse flux contribution of resolved gamma-ray blazars and TDEs to no more than 30% (Aartsen et al. 2017a) and 26% (Stein 2019), respectively, leaving the majority of the diffuse flux unexplained.

In general, high-energy neutrinos are created through interactions of high-energy protons with ambient matter or photon fields. Charged and neutral pions produced in those interactions decay to neutrinos and gamma-rays, respectively. While gamma-rays can also be produced in leptonic processes such as inverse Compton scattering, neutrinos are considered to be a clear signature for hadronic interactions and thus also cosmic-ray acceleration.

Several source classes have been proposed as candidate neutrino (and cosmic-ray) sources. Among the most promising are active galactic nuclei, gamma-ray bursts (GRBs) and supernovae (SNe)—see Kurahashi et al. (2022) for a recent review. While gamma-bright GRBs are strongly disfavored as the main contributor to the measured diffuse neutrino flux (Aartsen et al. 2017b), a large population of nearby low-luminosity bursts could still contribute significantly. The discovery of a connection between GRBs and type Ic-BL SNe implies that (mildly) relativistic jets should also exist in a fraction of core-collapse SNe (Razzaque et al. 2004; Ando & Beacom 2005; Senno et al. 2016; Denton & Tamborra 2018), where such jets might be choked inside the envelope of the star. In this scenario, the gamma-rays would be absorbed but the neutrinos could still escape. A short neutrino burst (~ 100 s) would be expected, in coincidence with the explosion time of the SNe (Senno et al. 2016). Past analyses did not find significant correlation with high-energy neutrinos, and they put

model-dependent constraints on the fraction of supernovae type Ibc with a choked jet and the energy emitted in cosmic-rays (Esmaili & Murase 2018; Senno et al. 2018).

Another possibility for producing high-energy neutrinos in core-collapse supernovae (CCSNe) is through interactions of the SN ejecta with a dense circumstellar medium (CSM). Strong stellar winds in the star’s late evolution stages or pre-outburst could produce a sufficiently dense CSM (Ofek et al. 2013; Strotjohann et al. 2021). When the supernova shock front reaches this dense medium, efficient acceleration of charged particles on timescales ranging from a few tens of seconds to ~ 1000 days may occur (Murase et al. 2011; Zirakashvili & Ptuskin 2016; Sarmah et al. 2022). CSM interactions can be revealed through the detection of a combination of narrow and broad emission lines (as observed in type IIn SNe). The narrow component of the spectral lines is produced by circumstellar gas, which is ionized as the shock breaks out of the star. The intermediate and broad components are produced by shocked, high-velocity SN ejecta, arising as a result of the collision of the ejecta with circumstellar gas. Another indication might be a long plateau in the SN light curve (as seen in Type IIP SNe), which could be partly powered by SN shock breakout interaction with dense CSM (Moriya et al. 2011, 2012). Some IIP SNe show direct observational evidence for interactions (Mauerhan et al. 2013; Faran et al. 2014; Yaron et al. 2017; Nakaoka et al. 2018). Studies find IIP supernovae to be viable candidates for neutrino production through interactions with the CSM (Murase 2018; Sarmah et al. 2022). Pitik et al. (2022) found the high-energy neutrino IC200530A in spatial coincidence with the optical transient AT2019fdr, which they interpret as a Type IIn superluminous supernova.

Optical follow-up campaigns of IceCube high-energy neutrino alerts (Necker et al. 2022; Stein et al. 2022b) are close to constraining the brightest observed superluminous supernovae.

Here, for the first time, we probe different SN classes as potential neutrino sources and calculate their possible contribution to the observed diffuse neutrino flux. To search for cross-correlation between neutrinos and optically observed SNe, we utilize data recorded by the IceCube Neutrino Observatory.

This paper is organized as follows: Section 2 describes the relevant data sets, followed by a discussion of the analysis methods in Section 3 and the presentation of the results in Section 4. Section 5 presents the constraints on the contribution of CCSNe to the diffuse neutrino flux. Section 6 summarizes the paper. Upper limits on the total energy released in neutrinos from individual SNe can be found in Appendix C.

2. The Data

IceCube is a cubic-kilometer-sized neutrino detector, located in the transparent ice of the 2.8 km thick glacier covering the bedrock at the geographical South Pole (Aartsen et al. 2017c). Neutrino–nucleon interactions in the ice are detected indirectly, via Cherenkov light emission from secondary particles, by 5160 photomultiplier tubes. While charged-current interactions of muon neutrinos produce track-like signatures with subdegree angular resolution, both charged-current interactions of electron and tau neutrinos as well as neutral-current interactions have angular resolutions of several degrees. This analysis utilizes a selection of seven years of IceCube muon-track data that were optimized for point-source searches (Aartsen et al. 2017d), with roughly 700,000 events from years 2008 to 2014.

The CCSN catalog for this analysis was compiled using publicly available records of optical detections of SNe. The primary sources were the WiseREP SN catalog (Yaron & Gal-Yam 2012) and the OpenSupernovaCatalog (Guillochon et al. 2017). In total, the compiled source sample contains 339 type IIIn SN, 198 type IIP SN, and 503 type Ib/c and type IIb SNe. The latter are referred to as stripped-envelope supernovae. Both type IIIn and type IIP SN are candidates for CSM interaction, while stripped-envelope supernovae might host choked jets. In Figure 1, the distance distribution of the two subsamples is shown. It should be noted that, while we did include many supernovae in the analysis, we list only those of a smaller subsample in Appendix A, as explained below.

The distance was taken from the previously cited catalogs. For cases in which entries were missing in the catalogs, the distances were estimated using redshift measurements. The Λ CDM model, with cosmological parameters measured by Planck (Ade et al. 2016), was used to convert from redshift to luminosity distance. We have assumed a peculiar motion of $[300] \text{ km s}^{-1}$, which also provides a lower distance limit for SNe with very small redshifts. SNe with neither distance nor redshift measurements were excluded from the catalog. The distance distribution peaks at about $[100] \text{ Mpc}$, as can be seen in Figure 1.

3. Analysis Method

To find an excess of neutrinos from the given SN positions and times, a time-dependent point-source likelihood method (Braun et al. 2010) is used. The likelihood function is given by

$$\mathcal{L} = \prod_{i=1}^N \left(\frac{n_s}{N} \mathcal{S}(\nu_i) + \left(1 - \frac{n_s}{N} \right) \mathcal{B}(\nu_i) \right), \quad (1)$$

where N is the number of neutrino events, ν_i is the i th neutrino, and n_s is the number of signal events. \mathcal{S} and \mathcal{B} are signal and background probability distribution functions (PDFs). Each PDF is a product of a spatial term \mathcal{N} , an energy term \mathcal{E} , and a time term \mathcal{T} , which for the signal PDF can be expressed as

$$\mathcal{S} = \mathcal{N}_S \times \mathcal{E}_S(\gamma) \times \mathcal{T}_S, \quad (2)$$

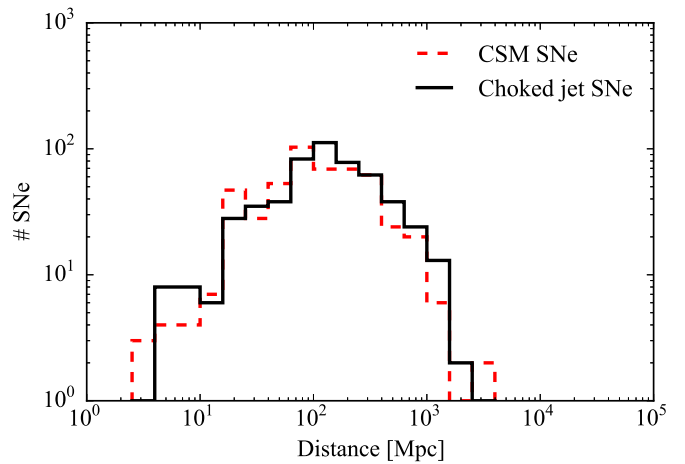


Figure 1. Distance distribution of CSM SN sample and the stripped-envelope SN sample. The decrease at large distance is a result of limited detection sensitivity and a selection bias toward brighter objects, which are easier to classify spectroscopically.

and the background PDF \mathcal{B} is calculated similarly (Braun et al. 2010). The signal time PDF \mathcal{T}_S corresponds to the expected neutrino flux as a function of time (light curve), and the background time PDF \mathcal{T}_B assumes a constant background rate.

The energy term \mathcal{E} describes the expected neutrino energy spectrum. As the data set is highly background-dominated,⁶⁹ we can safely assume that the signal contribution is negligible. The background energy proxy distribution is thus assumed to follow the distribution observed in the data. The signal neutrino energy distribution is described as a power-law function, $E^{-\gamma}$, where γ is the spectral index. For similar reasons, the background spatial PDF as a function of decl. is chosen to match the distribution of declinations found in the data. We assume that the background spatial PDF is uniform in R.A., leading to $\mathcal{N}_B(\delta, \phi) = \frac{1}{2\pi} \times \mathcal{N}_{B,\text{dec}}(\delta)$ for source decl. δ and R.A. ϕ . The signal spatial PDF, \mathcal{N}_S , is assumed to follow a 2D Gaussian distribution.

The likelihood function is maximized with respect to n_s and γ . The best-fitted value n_s gives an estimate of the number of signal-like events, i.e., those that are likely to originate from a given SN.

We define the test statistic (TS) by

$$\lambda = 2 \times \log \left(\frac{\mathcal{L}(\hat{n}_s, \hat{\gamma})}{\mathcal{L}(0)} \right), \quad (3)$$

where $\mathcal{L}(\hat{n}_s, \hat{\gamma})$ corresponds to the maximum of the likelihood function and $\mathcal{L}(0)$ to the null hypothesis, i.e., the case of neither spatial nor temporal correlation of neutrinos and SNe (Braun et al. 2008, 2010).

In principle, λ should follow a χ^2 -distribution (Wilks 1938), in which case we could just use its analytical form to describe the background distribution of the test statistic. However, in practice we constrain n_s to be positive and n_s and γ are not independent, which causes deviations from the χ^2 distribution. So instead, we estimate the background test statistic distribution by generating

⁶⁹ For an astrophysical signal component in the data set with a spectral index of $\gamma=2.5$, we expect $\mathcal{O}(10^3)$ signal events and $\mathcal{O}(10^5)$ atmospheric background events, amounting to a signal contribution of $<1\%$.

background-only pseudo-data sets and maximize the likelihood function with respect to n_s and γ . To be conservative and to avoid mismatches between simulations and data, we generate these data sets directly from the data. Because IceCube is located at the South Pole, the distribution of the data in R.A. is uniform and the background pseudo-data sets can be generated by randomly sampling values for the R.A. and shuffling the times of the neutrino events. This scrambling method is well established and preserves the structure in energy and decl. (see, e.g., Braun et al. 2008; Abbasi et al. 2022a, 2022b, 2022c).

Given an experimental outcome λ_{exp} and the background test statistic distribution $P(\lambda)$, the p -value is computed as $p = \int_{\lambda_{\text{exp}}}^{\infty} P(\lambda) d\lambda$.

In addition to probing the neutrino fluxes from single SNe, we combine the signal of a sample of SNe with a stacking analysis. Such a source stacking is implemented through a weighted sum of the signal PDFs \mathcal{S}_j of individual SNe j :

$$\mathcal{S} = \sum_j w_j \mathcal{S}_j, \quad (4)$$

where the weights w_j represent the expected signal strength of the sources. In this analysis, the weights are assumed to be proportional to

$$w_j \propto \underbrace{\frac{\Phi_0}{D_p^2}}_{\text{Source Properties}} \times \underbrace{\int_{t_{\text{start}}}^{t_{\text{end}}} \int_{E_{\text{min}}}^{E_{\text{max}}} L_j^\nu E^{-\gamma} A_{\text{eff}} dt dE}_{\text{Time Dependence}}, \quad (5)$$

with Φ_0 as the intrinsic neutrino power of the sources, D_p as the proper distance (Hogg 1999) of the SN, $L_j^\nu(t)$ the estimated neutrino light curve, $E^{-\gamma}$ the neutrino energy spectrum, and $A_{\text{eff}}(t, \delta_j, E)$ the effective area, the energy E , and the decl. of the source δ . The effective area is time-dependent, because the data set covers several distinct phases of detector construction. The weighting scheme assumes a standard candle ansatz, since we assume the same Φ_0 for each source. It is very sensitive to the estimated source distances, which can have large uncertainties.

A more detailed investigation of the supernova light curves could mitigate these uncertainties, but the optical light curves of the supernovae in our catalog are typically sparse and make detailed modeling complicated. Wrongly estimated weights will impact the sensitivity of the analysis, so for the first time in an IceCube analysis, we use a novel method of directly fitting the weights w_j . Adding the flux per source as an additional free parameter to the maximum likelihood removes the standard candle assumption and also the dependence on the SN distance estimate, but it requires a more advanced numerical procedure to maximize the likelihood function. To test the power of this method, we simulated five sources with random positions on the sky and respective weights. We then perturbed the weights according to a log-normal distribution and used them to compute the sensitivity of the standard, fixed-weights likelihood. Comparing to this, we find an improvement of up to 40% when using the fitting-weights likelihood. We applied this method in addition to the traditional standard candle one, yielding two separate results.

4. Constraints on Supernova Subclasses

In the following, we present results for selected individual CCSNe, as well as for different subclasses of CCSNe.

Stripped-envelope SNe, which might have choked jets, are expected to emit a short burst of neutrinos in coincidence with the SN explosion time (Senno et al. 2016). Motivated by theoretical uncertainties in the duration of the expected neutrino emission—and even larger uncertainties in the SNe explosion time, due to sparse optical light-curve data—we used a box function starting at 20 days before and extending up to the first available optical data. This ensures the inclusion of the explosion time for a typical SN even if the first detection happened at peak time.

All SN types were tested with box function PDFs of length 100, 300, and 1000 days, starting at the first available optical data, because longer neutrino emission would be expected under the scenario of CSM interaction. In addition, for SNe IIn and IIP, light curves were tested of the form:

$$\mathcal{T}(t) \propto \left(1 + \frac{t}{t_{\text{pp}}}\right)^{-1}, \quad (6)$$

where values of 0.02, 0.2, and 2 yr were used for the characteristic timescale constant t_{pp} , as proposed by Zirakashvili & Ptuskin (2016).

We first applied the maximum likelihood method described above to a selection of individual SNe, which were identified based on their expected relative signal strength w_j as promising. We did not find a statistically significant excess for any of the selected sources.

The resulting upper limits on the total energy emitted in neutrinos between $[10^2]$ GeV and $[10^7]$ GeV, assuming an E^{-2} power-law spectrum, are presented in Appendix C. In the conversion from the number of neutrino events to flux, the systemic uncertainty is estimated to be about 11%, mainly arising from uncertainties in the optical properties of the ice and detector effects (Coenders 2016).

The individual upper limits range from 10^{49} to 6.5×10^{50} erg,⁷⁰ which corresponds to 1%–65% of the typical bolometric electromagnetic energy released in SNe. As the individual stripped-envelope and IIP SNe are typically closer than the IIn, we generally obtain more stringent limits for these objects.

In order to improve our sensitivity, we performed a stacking analysis, looking for a combined excess from a catalog instead of individual sources. As explained above, we separate supernovae into SNe type IIn, SNe type IIP, and stripped-envelope SNe. It is worth noting that we decided to treat types IIn and IIP separately because the presence of CSM interaction in IIP is less certain.

Each of the three subcatalogs was split into two samples: a bright sample of nearby sources, containing about 70% of the expected signal; and a larger sample, containing the remaining dimmer sources. The bright samples include about 10 SN each, depending on the SN class and the model. The catalogs of the bright samples are listed in Appendix A. Testing both samples independently allowed us to benefit from the better optical observations of the nearby sources in the small sample but also utilize the larger statistics in the large sample. Because each source adds a free parameter in the likelihood maximization when fitting the weights, this was only feasible for the smaller

⁷⁰ Calculated by integrating over time.

bright sample. This sample contains $\mathcal{O}(10)$ sources, which is a manageable amount of fit parameters. For the large sample, the standard candle ansatz was applied instead.

The p -values are given in Appendix B. The most significant pre-trial p -value is 0.62%, and it is found in the search for neutrinos from the large sample of type IIP SNe in a 1000 day-long box-shaped light curve. However, this corresponds to a post-trial p -value of 19.5%, after accounting for the multiple tested scenarios through simulated pseudo-experiments of the ensemble of p -values, and it is thus consistent with background expectations. If this excess were due to astrophysical neutrinos, one would expect a corresponding excess in the sample of nearby type IIP SNe, where we do not find such an excess. The second-smallest p -value of 6.3% is found for the nearby type IIn SNe in the case of the fitted weights for the box-shaped light-curve model. The overall deviation of all tested scenarios from the background expectation using a Kolmogorov–Smirnov test leads to a p -value of 29%.

To be conservative, we use the result from the fitting-weights analysis in the rest of the paper, as it resulted in weaker upper limits on the total emitted neutrino energy. Including systematic uncertainties, those are shown in Figure 2 for both models of the neutrino light curve. These limits assume that SNe within each category behave as neutrino standard candles.

The stacking result provides us with stronger limits than individual source limits. We find that SNe type IIn emit less than 1.3×10^{49} erg and type IIP less than 2.4×10^{48} erg, while the strongest limits for stripped-envelope SNe of 4.5×10^{48} erg are obtained from the choked-jet scenario. If the longer box models that are associated with CSM interaction are assumed, then the strongest limit becomes 2.7×10^{48} erg. In general, the box time window provides tighter constraints for CSM-interacting SNe compared to the specific light-curve model of Zirakashvili & Ptuskin (2016).

5. Diffuse Neutrino Flux

Using the limits on neutrino energy obtained in the stacking analysis (shown in Figure 2), we can estimate the maximal contribution from the entire cosmological population of SNe to the measured diffuse neutrino flux (Aartsen et al. 2015). Using the CCSNe rate density found by Strolger et al. (2015), $\dot{\rho}(z)$, the diffuse flux is computed following the procedure in Ahlers & Halzen (2014) assuming a 1:1:1 (ν_e : ν_μ : ν_τ) neutrino flavor ratio at Earth. It is worth noting that we assume the rate for the individual subclasses scales according to the corresponding percentage in the local Universe (Li et al. 2011). The diffuse flux is given by

$$\phi(E) = \frac{1}{4\pi} \int_0^\infty \frac{\dot{\rho}(z)}{1+z} \frac{dN}{dE} \frac{c}{H(z)} dz, \quad (7)$$

where dN/dE is the time-integrated spectral density upper limit for each SN subclass, assuming that the subclass behaves as a neutrino standard candle class with a power-law energy spectrum and that the power law holds over our sensitive energy range. This energy range is calculated by finding the energy bound for selecting simulated signal events. We find the values where our sensitivity drops by 5% for the lower and upper bounds separately. The range between both values is our 90% energy range.

The resulting upper limits on the contribution of different SN types to the diffuse neutrino flux are shown in the bottom panel

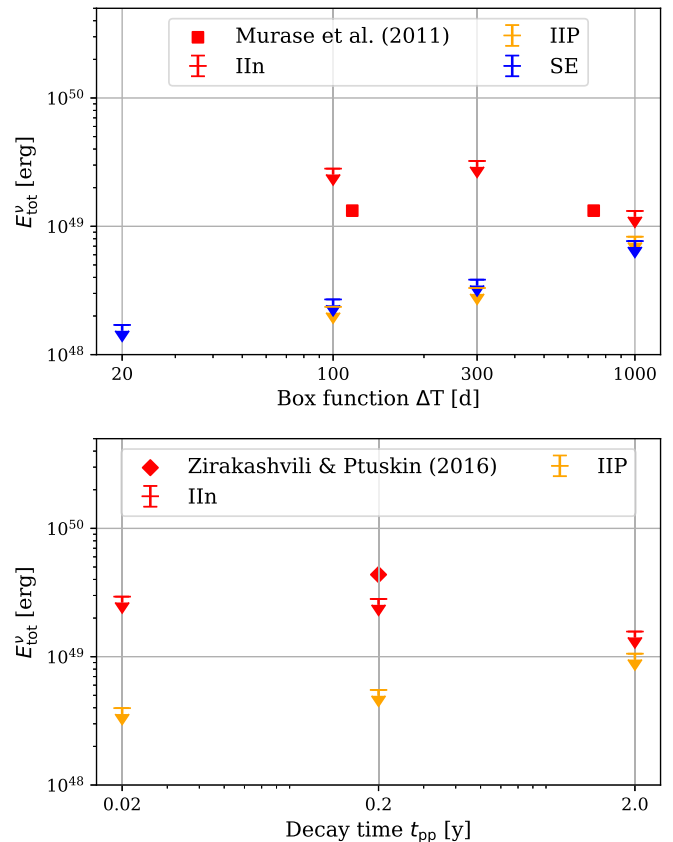


Figure 2. Upper limits on total neutrino ($\nu_\mu + \bar{\nu}_\mu$) energy assuming a box-like neutrino light curve (upper panel) and assuming a $L_\nu \propto \left(1 + \frac{t}{t_{pp}}\right)^{-1}$ neutrino light curve as predicted by Zirakashvili & Ptuskin (2016). The energy ranges are the same as indicated in Figure 3. The model predictions by Murase et al. (2011) and Zirakashvili & Ptuskin (2016) are shown as red squares for comparison.

of Figure 3 for a spectral index of $\gamma = 2.0$ as motivated by theoretical models (Murase 2018; Sarmah et al. 2022). Following a data-driven approach, the top panel shows the limits for a spectral index of $\gamma = 2.5$ as motivated by the central value of the global fit diffuse neutrino flux (Aartsen et al. 2015). Assuming the choked-jet scenario, stripped-envelope SNe cannot contribute more than 14.6% of the observed diffuse neutrino flux. Assuming interaction with the CSM, stripped-envelope SNe and SNe type IIn can explain no more than 26.6% and 33.9%, respectively. We mildly constrain the contribution of SNe type IIP to be less than 59.9%. We note that the limit for type IIP SNe seems weaker when translating it to a component of the diffuse flux, because they are the most abundant supernova type (Li et al. 2011).

For stripped-envelope SNe, this analysis is complementary to that of Chang et al. (2022), who take into account the fraction of supernovae f_{jet} that harbor a choked-jet pointing in our line of sight to arrive at a limit on the contribution to the diffuse flux that is about ten times less stringent. Because we assume the supernovae of each subclass to be standard candles when deriving the upper limits on the total emitted neutrino energy in Section 4, our results are robust for $f_{\text{jet}} \approx 1$ but they will be less stringent for $f_{\text{jet}} \ll 1$.

This analysis has different sensitivities for different energy ranges; see Figure 4. The region of greatest sensitivity is

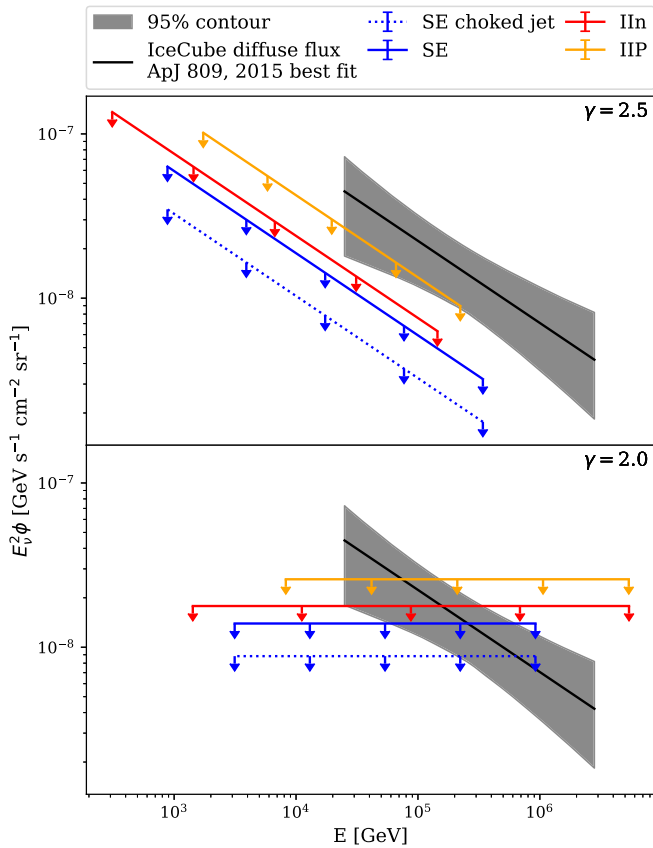


Figure 3. Upper limit on the contribution of different SN types to the diffuse neutrino flux ($\nu_\mu + \bar{\nu}_\mu$) assuming an $E^{-2.5}$ (top panel) and $E^{-2.0}$ (bottom panel) energy spectrum compared with the measured diffuse astrophysical neutrino flux (gray band). The limits are derived from the corresponding strictest limit in Figure 2. The choked-jet model refers to the 20 day box model, as explained in Section 4. The energy range plotted here is the central 90% energy range of the analyzed neutrino sample.

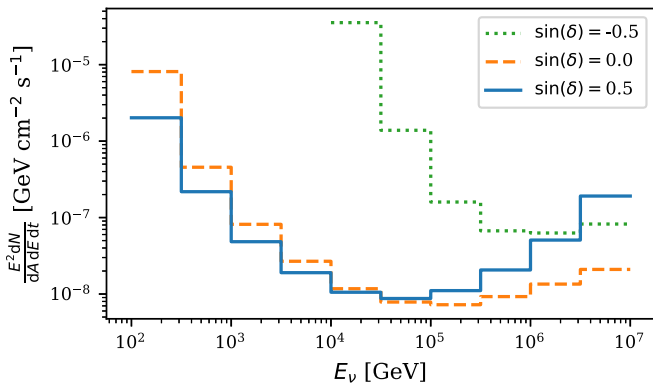


Figure 4. Differential sensitivity as a function of energy for different source declinations δ with one year of experimental data. The maximum sensitivity is achieved around $[10^5]$ GeV for sources located in the northern sky and close to the equator. For sources located in the southern sky, the overall sensitivity is much worse, but it also peaks at higher energies of $[10^6]$ GeV.

around 10–100 TeV. It can reach to higher energies as well, depending on the source decl. This broadly overlaps with the energy range in which the diffuse IceCube neutrino flux global fit was measured. The quoted upper limits to the diffuse flux contribution are thus not strongly dependent on the extrapolation of the measured diffuse flux to lower energies, where the flux has not yet been measured due to large atmospheric background.

6. Conclusion

We have presented a search for neutrinos from certain types of CCSNe with IceCube. In a stacking analysis, we correlated more than 1000 SNe from optical surveys with roughly 700,000 muon-track events recorded by IceCube. The standard stacking method was extended to allow for fitting of individual weights for each source, in order to account for expected variation in the neutrino flux from individual sources. Type IIn SNe, type IIP SNe, and stripped-envelope SNe were tested individually with various neutrino emission time models. No significant temporal and spatial correlation of neutrinos and the cataloged SNe was found, allowing us to set upper limits on the contribution of those SNe to the diffuse neutrino flux.

Type IIn CCSNe, type IIP CCSNe, and stripped-envelope SNe contribute less than 34%, 60%, and 27%, respectively, to the diffuse neutrino flux at the 90% confidence level, assuming CSM interaction and an extrapolation of the diffuse neutrino spectrum to low energies following an unbroken power law with index -2.5 . This also assumes a choked-jet, stripped-envelope SNe cannot contribute more than 15%.

Upper limits on the total neutrino energy emitted by a single CSM-interacting source are at levels comparable to model predictions by Murase et al. (2011) (see Figure 2), while model predictions from Zirakashvili & Ptuskin (2016) are strongly disfavored. It should be noted that the model prediction could easily be adjusted to lower neutrino flux predictions by assuming a lower CSM density or a lower kinetic SN energy.

Improvements to the presented limits are expected in the near future with optical survey instruments such as the Zwicky Transient Factory (Graham et al. 2019), which is able to undertake a high-cadence survey across a large fraction of the sky, providing SN catalogs with much greater completeness. In combination with next-generation neutrino telescopes, this will significantly boost the sensitivity of this type of analysis, allowing us to probe dimmer neutrino emitters and smaller contributions of CCSNe to the diffuse neutrino flux.

The IceCube collaboration acknowledges the significant contributions to this manuscript from Jannis Necker, Alexander Stasik, and Robert Stein. We also gratefully acknowledge support from: USA—the U.S. National Science Foundation—Office of Polar Programs, the U.S. National Science Foundation—Physics Division, the U.S. National Science Foundation—EPSCoR, the Wisconsin Alumni Research Foundation, the Center for High Throughput Computing (CHTC) at the University of Wisconsin—Madison, the Open Science Grid (OSG), Advanced Cyberinfrastructure Coordination Ecosystem: Services & Support (ACCESS), the Frontera computing project at the Texas Advanced Computing Center, the U.S. Department of Energy—National Energy Research Scientific Computing Center, the Particle Astrophysics Research Computing Center at the University of Maryland, the Institute for Cyber-Enabled Research at Michigan State University, and the Astroparticle Physics Computational Facility at Marquette University; Belgium—Funds for Scientific Research (FRS-FNRS and FWO), the FWO Odysseus and Big Science programmes, and the Belgian Federal Science Policy Office (Belspo); Germany—Bundesministerium für Bildung und Forschung (BMBF), Deutsche Forschungsgemeinschaft (DFG), Helmholtz Alliance for Astroparticle Physics (HAP), the Initiative and Networking Fund of the Helmholtz Association, Deutsches Elektronen Synchrotron (DESY), and the High

Performance Computing Cluster of the RWTH Aachen; Sweden—the Swedish Research Council, the Swedish Polar Research Secretariat, the Swedish National Infrastructure for Computing (SNIC), and the Knut and Alice Wallenberg Foundation; European Union—EGI Advanced Computing for Research; Australia—the Australian Research Council; Canada—the Natural Sciences and Engineering Research Council of Canada, Calcul Québec, Compute Ontario, the Canada Foundation for Innovation, WestGrid, and Compute Canada; Denmark—Villum Fonden, the Carlsberg Foundation, and the European Commission; New Zealand—the Marsden Fund; Japan—the Japan Society for Promotion of Science (JSPS) and the Institute for Global Prominent Research (IGPR) of Chiba University; Korea

—the National Research Foundation of Korea (NRF); Switzerland—the Swiss National Science Foundation (SNSF); United Kingdom—Oxford University, Department of Physics.

Facilities: HST(STIS), Swift(XRT and UVOT), AAVSO, CTIO:1.3 m, CTIO:1.5 m, CXO.

Software: flarestack (Stein et al. 2022a).

Appendix A Catalogs

Tables 1, 2, and 3 list the supernova catalogues used in the fitting weights analysis as described in Section 4.

Table 1
Interacting Supernovae Catalog

Name	R.A. (rad)	Decl. (rad)	Discovery Date	Redshift	Distance (Mpc)	Source
SN1999bw	2.70	0.79	1999-00-20	0.0032	9.80	1, 2
SN2002bu	3.22	0.80	2002-00-28	0.0030	8.90	1, 2, 3
SN2008S	5.39	1.05	2008-00-01	0.0012	5.60	4
SN2009kr	1.36	-0.27	2009-00-06	0.0075	16.00	5
SN2010jl	2.54	0.17	2010-00-03	0.0117	49.00	6
SN2011an	2.09	0.29	2011-00-01	0.0170	73.00	7
SN2011ht	2.65	0.90	2011-00-29	0.0046	19.20	8
SN2012ab	3.24	0.10	2012-00-31	0.0190	81.00	9
SN2013by	4.29	-1.05	2013-00-23	0.0038	14.80	10, 11
SN2013gc	2.13	-0.49	2013-00-07	0.0044	15.10	12
PSN J14041297-0938168	3.68	-0.17	2013-00-20	0.0038	12.55	13
CSS140111:060437-123740	1.59	-0.22	2013-00-24	0.0084	32.88	13
SN2014G	2.86	0.95	2014-00-14	0.0045	20.00	14
MASTER OT J044212.20+230616.7	1.23	0.40	2014-00-21	0.0170	72.00	15
SN2015da	3.63	0.69	2015-00-09	0.0079	32.14	16, 17

References. (1) Kochanek et al. 2012; (2) Smith et al. 2011; (3) Szczygielet al. 2012; (4) Stanishev et al. 2008; (5) Steele et al. 2009a; (6) Benetti et al. 2010; (7) Marion & Calkins 2011; (8) Prieto et al. 2011; (9) Bilinski et al. 2018; (10) Margutti et al. 2013; (11) Parker et al. 2013; (12) Antezana et al. 2013; (13) Challis 2013; (14) Denisenko et al. 2014; (15) Shivvers et al. 2014; (16) Zhang & Wang 2015; (17) Tartaglia et al. 2020.

Table 2
IIP Catalog

Name	R.A. (rad)	Decl. (rad)	Discovery Date	Redshift	Distance (Mpc)	Source
SN1999em	1.23	-0.05	1999-00-29	0.0034	7.50	1
SN2004dj	2.00	1.14	2004-00-31	0.0014	3.50	2
SN2004et	5.39	1.05	2004-00-27	0.0022	7.70	3, 4
SN2005cs	3.53	0.82	2005-00-28	0.0030	7.10	5, 6
SN2006ov	3.24	0.08	2006-00-24	0.0062	14.00	7
SN2008bk	6.27	-0.57	2008-00-25	0.0018	4.00	8
SN2009js	0.64	0.32	2009-00-11	0.0060	16.00	9
SN2009md	2.83	0.22	2009-00-05	0.0046	18.00	10
SN2009mf	0.27	0.83	2009-00-07	0.0087	23.00	11
SN2011dq	0.26	-0.13	2011-00-15	0.0055	24.40	12
SN2012A	2.73	0.30	2012-00-07	0.0034	9.80	13
SN2012aw	2.81	0.20	2012-00-16	0.0036	9.90	14
SNhunt141	3.57	-0.31	2012-00-24	0.0040	18.00	15
SN2012ec	0.72	-0.13	2012-00-12	0.0057	18.76	16
SN2013ab	3.81	0.17	2013-00-17	0.0063	23.64	17
SN2013am	2.96	0.23	2013-00-21	0.0037	12.77	18
SN2013bu	5.92	0.60	2013-00-21	0.0027	12.07	19
SN2013ej	0.42	0.28	2013-00-25	0.0020	9.00	20
SN2011ja	3.43	-0.86	2014-00-14	0.0018	3.36	21
SN2014bc	3.22	0.83	2014-00-19	0.0025	7.60	22

References. (1) Jha et al. 1999; (2) Patat et al. 2004; (3) Zwitter et al. 2004; (4) Li et al. 2005; (5) Modjaz et al. 2005; (6) Pastorello et al. 2009; (7) Li et al. 2007; (8) Morrell & Stritzinger 2008; (9) Gandhi et al. 2013; (10) Sollerman et al. 2009; (11) Steele et al. 2009b; (12) Valenti & Benetti 2011; (13) Stanishev & Pursimo 2012; (14) Quadri et al. 2012; (15) Cellier-Holzem et al. 2012; (16) Monard et al. 2012; (17) Bose et al. 2015; (18) Benetti et al. 2013; (19) Itagaki et al. 2013; (20) Dhungana et al. 2016; (21) Andrews et al. 2016; (22) Ochner et al. 2014.

Table 3
Stripped-envelope Supernovae Catalog

Name	R.A. (rad)	Decl. (rad)	Discovery Date	Redshift	Distance (Mpc)	Source
SN2007gr	0.71	0.65	2007-00-15	0.0027	9.30	1, 2
SN2008ax	3.28	0.73	2008-00-03	0.0029	9.60	3, 4
SN2008dv	0.95	1.27	2008-00-01	0.0084	4.20	5
SN2009dq	2.66	-1.17	2009-00-24	0.0046	16.00	6
SN2009gj	0.13	-0.58	2009-00-21	0.0053	17.00	7
SN2009mk	0.03	-0.72	2009-00-15	0.0050	22.00	8, 9
SN2009mu	2.58	-0.58	2009-00-21	0.0098	25.00	10
SN2010br	3.16	0.78	2010-00-10	0.0033	13.00	11
SN2010gi	4.55	1.32	2010-00-18	0.0041	18.20	12
SN2011dh	3.53	0.82	2011-00-01	0.0025	8.40	5
SN2011jm	3.38	0.05	2011-00-24	0.0041	14.00	13
SN2012P	3.93	0.03	2012-00-22	0.0055	20.10	14, 15
SN2012cw	2.68	0.06	2012-00-14	0.0055	19.92	16, 17
SN2012fh	2.81	0.43	2012-00-18	0.0029	8.58	18, 19, 20
SN2013df	3.26	0.55	2013-00-07	0.0033	10.58	21, 22
iPTF13bvn	3.93	0.03	2013-00-17	0.0055	19.94	15, 23, 24, 25
MASTER OT J120451.50+265946.6	3.16	0.47	2013-00-02	0.0029	8.38	26, 27, 28
SN2013ge	2.77	0.38	2013-00-08	0.0054	19.34	29, 30
SN2014C	5.92	0.60	2014-00-05	0.0037	12.07	31, 32, 33

References. (1) Chornock et al. 2007; (2) Valenti et al. 2008; (3) Chornock et al. 2008; (4) Pastorello et al. 2008; (5) Silverman et al. 2008; (6) Anderson et al. 2009; (7) Stockdale et al. 2009; (8) Chornock & Berger 2009; (9) Marples & Drescher 2009; (10) Stritzinger et al. 2010; (11) Maxwell et al. 2010; (12) Yamanaka et al. 2010; (13) Foley & Fong 2011; (14) Borsato et al. 2012; (15) Fremling et al. 2016; (16) Itagaki et al. 2012; (17) Wang et al. 2012; (18) Johnson et al. 2017; (19) Takaki et al. 2012; (20) Tomasella et al. 2012; (21) Ciabattari et al. 2013; (22) Van Dyk et al. 2014; (23) Cao et al. 2013; (24) Milisavljevic et al. 2013; (25) Srivastav et al. 2014a; (26) Chandra et al. 2019; (27) Singh et al. 2019; (28) Srivastav et al. 2014b; (29) Drout et al. 2016; (30) Nakano et al. 2013; (31) Kim et al. 2014; (32) Milisavljevic et al. 2015; (33) Tinyanont et al. 2016.

Appendix B

P-values [%]

Table 4 lists the pre-trial *P*-values of the fitted weights scenario given as percentages for a box-shaped light-curve

model of different length and for the CSM model of Zirakashvili & Ptuskin (2016) for different choices of t_{pp} .

Table 4
Pre-trial *P*-values

	Box Length (days)				t_{pp} (yr)		
	[-20, 0]	[0, 100]	[0, 300]	[0, 10000]	0.02	0.2	2.0
IIn	...	8.6	6.3	>50	>50	>50	30.1
IIP	...	48.6	>50	27.6	>50	>50	21.6
Stripped-envelope	>50	>50	>50	34.8

Appendix C Upper Limits on Individual Sources

This section shows upper limits on individual SNe. Sources were selected based on their expected neutrino signal. Here, we

assume a generic neutrino energy spectrum of E^{-2} , rather than tying them to the observed diffuse spectral shape, and an emission time window of 100 days. Table 5 lists IIc SNe, Table 6 IIP SNe, and Table 7 the stripped-envelope SNe.

Table 5
Upper Limits on Selected Type IIc SNe

Name	R.A. (rad)	Decl. (rad)	Discovery Date	Distance (Mpc)	Energy Upper Limit (10^{49} erg)
CSS140111:060437-123740	1.59	-0.22	2013-12-24	31.8	49.8
PSN J13522411+3941286	3.63	0.693	2015-01-09	32.1	16.8
PSN J14041297-0938168	3.68	-0.168	2013-12-20	12.5	4.8
PTF10aaxf	2.54	0.166	2010-11-03	52.3	29.5
SN2008S	5.39	1.049	2008-02-01	5.6	5.3
SN2009kr	1.36	-0.274	2009-11-06	16.0	19.1
SN2011an	2.09	0.287	2011-03-01	73.0	65.3
SN2011ht	2.65	0.905	2011-09-29	19.2	6.6
SN2012ab	3.24	0.098	2012-01-31	81.0	64.18
SN2013gc	2.13	-0.49	2013-11-07	15.1	28.4

Table 6
Upper Limits on Selected Type IIP SNe

Name	R.A. (rad)	Decl. (rad)	Discovery Date	Distance (Mpc)	Energy Upper Limit (10^{49} erg)
iPTF13aaz	2.96	0.228	2013-03-21	16.4	1.0
SN2012A	2.73	0.299	2012-01-07	9.0	1.0
SN2012aw	2.81	0.204	2012-03-16	9.6	1.0
SN2014bc	3.22	0.826	2014-05-19	7.6	3.0

Table 7
Upper Limits on Selected Stripped-envelope SNe (Ib/c and IIb)

Name	R.A. (rad)	Decl. (rad)	Discovery Date	Distance (Mpc)	Energy Upper Limit (10^{49} erg)
iPTF13bvn	3.93	0.033	2013-06-17	25.8	4.0
MASTER OT J120451.50	3.16	0.471	2014-10-28	15.0	1.0
PTF11eon	3.53	0.823	2011-06-01	8.0	1.1
SN2008ax	3.28	0.727	2008-03-03	5.1	1.6
SN2008dv	0.95	1.267	2008-07-01	10.6	1.2
SN2010br	3.16	0.777	2010-04-10	9.9	4.1
SN2011jm	3.38	0.046	2011-12-24	14.0	1.8
SN2012cw	2.68	0.06	2012-06-14	31.3	4.3
SN2012fh	2.81	0.434	2012-10-18	8.6	1.1
SN2013df	3.26	0.545	2013-06-07	10.6	1.7
SN2014C	5.92	0.601	2014-01-05	12.1	2.3

- Chandra, P., Nayana, A. J., Björnsson, C. I., et al. 2019, *ApJ*, **877**, 79
- Chang, P.-W., Zhou, B., Murase, K., & Kamionkowski, M. 2022, arXiv:2210.03088
- Chornock, R., & Berger, E. 2009, CBET, **2086**, 1
- Chornock, R., Filippenko, A. V., Li, W., et al. 2007, CBET, **1036**, 1
- Chornock, R., Filippenko, A. V., Li, W., et al. 2008, CBET, **1298**, 1
- Ciabattari, F., Mazzoni, E., Donati, S., et al. 2013, CBET, **3557**, 1
- Coenders, S. 2016, Dissertation, Technische Universität München, München
- Esmaili, A., & Murase, K. 2018, *JCAP*, **2018**, 008
- Faran, T., Poznanski, D., Filippenko, A. V., et al. 2014, *MNRAS*, **442**, 844
- Foley, R. J., & Fong, W. 2011, CBET, **2962**, 2
- Fremming, C., Sollerman, J., Taddia, F., et al. 2016, *A&A*, **593**, A68
- Gandhi, P., Yamanaka, M., Tanaka, M., et al. 2013, *ApJ*, **767**, 166
- Graham, M. J., Kulkarni, S. R., Bellm, E. C., et al. 2019, *PASP*, **131**, 1538
- Guillochon, J., Parrent, J., Kelley, L. Z., & Margutti, R. 2017, *ApJ*, **835**, 64
- Hogg, D. W. 1999, arXiv:astro-ph/9905116
- IceCube Collaboration, Abbasi, R., Ackermann, M., et al. 2022, *Sci*, **378**, 538
- Itagaki, K., Noguchi, T., Nakano, S., et al. 2012, CBET, **3148**, 1
- Itagaki, K., Noguchi, T., Nakano, S., et al. 2013, CBET, **3498**, 1
- Jha, S., Challis, P., Garnavich, P., et al. 1999, IAUC, **7296**, 2
- Johnson, S. A., Kochanek, C. S., & Adams, S. M. 2017, *MNRAS*, **472**, 3115
- Kim, M., Zheng, W., Li, W., et al. 2014, CBET, **3777**, 1
- Kochanek, C. S., Szczygieł, D. M., & Stanek, K. Z. 2012, *ApJ*, **758**, 142
- Kurahashi, N., Murase, K., & Santander, M. 2022, *ARNPS*, **72**, 365
- Li, W., Leaman, J., Chornock, R., et al. 2011, *MNRAS*, **412**, 1441
- Li, W., Van Dyk, S. D., Filippenko, A. V., & Cuillandre, J.-C. 2005, *PASP*, **117**, 121
- Li, W., Wang, X., Van Dyk, S. D., et al. 2007, *ApJ*, **661**, 1013
- Margutti, R., Soderberg, A., & Milisavljevic, D. 2013, ATel, **5106**, 1
- Marion, G. H., & Calkins, M. 2011, CBET, **2668**, 2
- Marples, P., & Drescher, C. 2009, CBET, **2080**, 1
- Mauerhan, J. C., Smith, N., Silverman, J. M., et al. 2013, *MNRAS*, **431**, 2599
- Maxwell, A. J., Graham, M. L., Parker, A., et al. 2010, CBET, **2245**, 2
- Milisavljevic, D., Fesen, R., Pickering, T., et al. 2013, ATel, **5142**, 1
- Milisavljevic, D., Margutti, R., Kamble, A., et al. 2015, *ApJ*, **815**, 120
- Modjaz, M., Kirshner, R., Challis, P., & Hutchins, R. 2005, IAUC, **8555**, 1
- Monard, L. A. G., Childress, M., Scalzo, R., Yuan, F., & Schmidt, B. 2012, CBET, **3201**, 1
- Moriya, T., Tominaga, N., Blinnikov, S. I., Baklanov, P. V., & Sorokina, E. I. 2011, *MNRAS*, **415**, 199
- Moriya, T. J., Tominaga, N., Blinnikov, S. I., Baklanov, P. V., & Sorokina, E. I. 2012, IAU Symp. 279, Death of Massive Stars: Supernovae and Gamma-Ray Bursts 7 ed. P. Roming, N. Kawai, & E. Pian, (San Francisco, CA: ASP), **54**
- Morrell, N., & Stritzinger, M. 2008, CBET, **1335**, 1
- Murase, K. 2018, *PhRvD*, **97**, 081301
- Murase, K., Thompson, T. A., Lacki, B. C., & Beacom, J. F. 2011, *PhRvD*, **84**, 043003
- Nakano, S., Kiyota, S., Masi, G., et al. 2013, CBET, **3701**, 1
- Nakaoka, T., Kawabata, K. S., Maeda, K., et al. 2018, *ApJ*, **859**, 78
- Necker, J., de Jaeger, T., Stein, R., et al. 2022, *MNRAS*, **516**, 2455
- Ochner, P., Tomasella, L., Benetti, S., et al. 2014, ATel, **6160**, 1
- Ofek, E. O., Sullivan, M., Cenko, S. B., et al. 2013, *Natur*, **494**, 65
- Parker, S., Kiyota, S., Morrell, N., et al. 2013, CBET, **3506**, 1
- Pastorello, A., Kasliwal, M. M., Crockett, R. M., et al. 2008, *MNRAS*, **389**, 955
- Pastorello, A., Valenti, S., Zampieri, L., et al. 2009, *MNRAS*, **394**, 2266
- Patat, F., Benetti, S., Pastorello, A., Filippenko, A. V., & Accituno, J. 2004, IAUC, **8378**, 1
- Pitlik, T., Tamborra, I., Angus, C. R., & Auchettl, K. 2022, *ApJ*, **929**, 163
- Prieto, J. L., McMillan, R., Bakos, G., & Grennan, D. 2011, CBET, **2903**, 1
- Quadri, U., Strabla, L., Girelli, R., et al. 2012, CBET, **3054**, 1
- Razzaque, S., Mészáros, P., & Waxman, E. 2004, *PhRvL*, **93**, 181101
- Reusch, S., Stein, R., Kowalski, M., et al. 2022, *PhRvL*, **128**, 221101
- Sarmah, P., Chakraborty, S., Tamborra, I., & Auchettl, K. 2022, *JCAP*, **2022**, 011
- Senno, N., Murase, K., & Meszaros, P. 2016, *PhRvD*, **93**, 083003
- Senno, N., Murase, K., & Mészáros, P. 2018, *JCAP*, **2018**, 025
- Shivvers, I., Kelly, P. L., Clubb, K. I., & Filippenko, A. V. 2014, ATel, **6487**, 1
- Silverman, J. M., Griffith, C. V., Filippenko, A. V., Chornock, R., & Li, W. 2008, CBET, **1447**, 1
- Singh, M., Misra, K., Sahu, D. K., et al. 2019, *MNRAS*, **485**, 5438
- Smith, N., Li, W., Silverman, J. M., Ganeshalingam, M., & Filippenko, A. V. 2011, *MNRAS*, **415**, 773
- Sollerman, J., Ergon, M., Inserra, C., et al. 2009, CBET, **2068**, 1
- Srivastav, S., Anupama, G. C., & Sahu, D. K. 2014a, *MNRAS*, **445**, 1932
- Srivastav, S., Sahu, D. K., & Anupama, G. C. 2014b, ATel, **6639**, 1
- Stanishev, V., Pastorello, A., & Pursimo, T. 2008, CBET, **1235**, 1
- Stanishev, V., & Pursimo, T. 2012, CBET, **2974**, 3
- Steele, T. N., Cobb, B., & Filippenko, A. V. 2009a, CBET, **2011**, 1
- Steele, T. N., Kandrashoff, M. T., & Filippenko, A. V. 2009b, CBET, **2070**, 1
- Stein, R. 2019, in Proc. 36th ICRC—PoS (ICRC2019), **358**, 1016
- Stein, R., Necker, J., Bradascio, F., & Garrappa, S. 2022a, icecube/flarestack: Titan v2.4.2, Zenodo, doi:10.5281/zenodo.6425740
- Stein, R., Reusch, S., Franckowiak, A., et al. 2022b, *MNRAS*, **521**, 5046
- Stein, R., van Velzen, S., Kowalski, M., et al. 2021, *NatAs*, **5**, 510
- Stockdale, C. J., Rentz, B., Vandrevalla, C. M., et al. 2009, IAUC, **9056**, 1
- Stritzinger, M., Folatelli, G., & Pignata, G. 2010, CBET, **2116**, 1
- Strolger, L.-G., Dahlen, T., Rodney, S. A., et al. 2015, *ApJ*, **813**, 93
- Strotjohann, N. L., Ofek, E. O., Gal-Yam, A., et al. 2021, *ApJ*, **907**, 99
- Szczygieł, D. M., Kochanek, C. S., & Dai, X. 2012, *ApJ*, **760**, 20
- Takaki, K., Itoh, R., Ueno, I., et al. 2012, CBET, **3263**, 3
- Tartaglia, L., Pastorello, A., Sollerman, J., et al. 2020, *A&A*, **635**, A39
- Tinyanont, S., Kasliwal, M. M., Fox, O. D., et al. 2016, *ApJ*, **833**, 231
- Tomasella, L., Turatto, M., Benetti, S., et al. 2012, CBET, **3263**, 2
- Valenti, S., & Benetti, S. 2011, CBET, **2749**, 2
- Valenti, S., Elias-Rosa, N., Taubenberger, S., et al. 2008, *ApJL*, **673**, L155
- Van Dyk, S. D., Zheng, W., Fox, O. D., et al. 2014, *AJ*, **147**, 37
- Wang, X. F., Liu, Q., Zhang, J. J., Zhang, T. M., & Brimacombe, J. 2012, CBET, **3148**, 2
- Wilks, S. S. 1938, *Ann. Math. Statist.*, **9**, 60
- Yamanaka, M., Arai, A., Sakimoto, K., Okushima, T., & Kawabata, K. S. 2010, CBET, **2384**, 1
- Yaron, O., & Gal-Yam, A. 2012, *PASP*, **124**, 668
- Yaron, O., et al. 2017, *NatPh*, **13**, 510
- Zhang, J., & Wang, X. 2015, ATel, **6939**, 1
- Zirakashvili, V. N., & Ptuskin, V. S. 2016, *Aph*, **78**, 28
- Zwitter, T., Munari, U., & Moretti, S. 2004, IAUC, **8413**, 1